
SKiP: SVM weighted by K-Nearest-Neighbors and class Probability for weakening outliers

Jeonghoon Park KangJun Lee Jaemin Kim Doyeol Oh
Department of Computer Science & Engineering, UNIST
{hoonably, suri7897, jm611, ohdoyeol}@unist.ac.kr *

1 Introduction

Outliers are a major concern in machine learning, as they can significantly degrade model performance. They can be broadly divided into two types: (1) well-labeled samples that lie far from the main data distribution (Feature outliers), and (2) mis-labeled samples caused by incorrect or incomplete labeling (Label outliers). Both types can distort the decision boundary, especially in Support Vector Machines (SVM) [1], which treat all samples equally in the loss term.

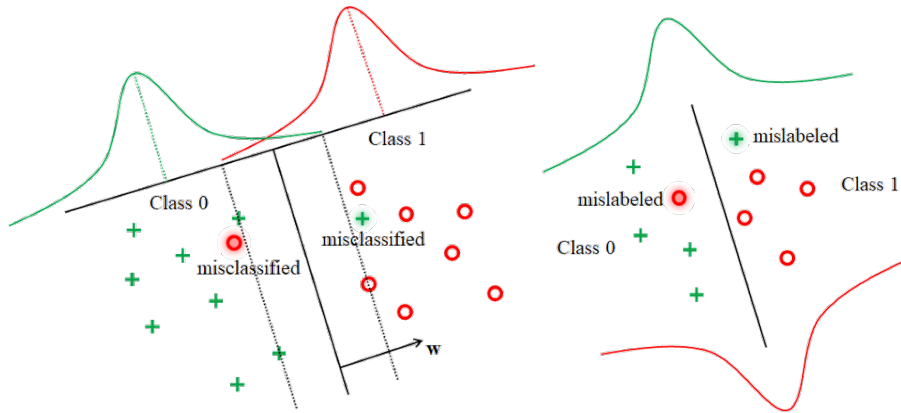


Figure 1: Two types of outliers: (Left) a correctly labeled sample far from the main distribution (Feature outliers), and (Right) a mislabeled sample near the decision boundary (Label outliers).

Traditional soft-SVM minimizes both the margin width and total hinge loss,

$$\min_{w,b} \frac{1}{2} \|w\|^2 + C \sum_i \xi_i, \quad (1)$$

subject to $y_i(w^\top x_i + b) \geq 1 - \xi_i$, $\xi_i \geq 0$,

but the penalty term $C \sum_i \xi_i$ does not differentiate between highly reliable samples and noise samples. Consequently, even a small number of outliers can significantly distort the separating hyperplane, as illustrated in Fig. 1, where both distant but correctly labeled samples and mislabeled boundary samples affect the decision boundary in undesirable ways.

To make SVM more robust against these two types of errors, we introduce SKiP, SVM weighted by K-Nearest-Neighbors and class Probability for weakening outliers. The core idea is to incorporate two complementary reliability measures into the slack penalty: a class-conditional probability p_i

*Codes are available on <https://github.com/hoonably/SKiP>

describing how well a sample aligns with the global distribution of its class, and a KNN-based label consistency measure n_i capturing how well its label agrees with that of its local neighbors. Whereas p_i is effective for identifying Feature outliers that lie far from the distribution, n_i provides sensitivity to labeling errors that occur near the margin.

Instead of multiplying these two terms, we adopt a stable additive design and define the sample-dependent penalty coefficient as

$$C_i = C \cdot \frac{p_i + n_i}{2}.$$

This formulation encourages the SVM to assign lower influence to samples that are globally unlikely or locally inconsistent, thereby jointly addressing both distributional outliers and mislabeled boundary points. By combining global probability informatn with local label consistency in a balanced manner, SKiP offers a robust and unified extension of soft-SVM capable of mitigating both label and feature outliers effectively.

2 Related Work

There have been several attempts to adapt the constant C in SVMs by assigning sample-dependent weights to the slack penalties. One representative line of work is the Fuzzy SVM (FSVM) [2] by Lin Wang, where each sample is assigned a fuzzy membership that reflects its reliability. While FSVM reduces the influence of noisy samples, its membership values are typically determined heuristically or through global distance-based criteria, and thus it does not explicitly incorporate local label consistency.

For another approach, Platt introduced the probability-weighted SVM [3], which modifies the slack coefficient using class-conditional probabilities typically obtained through sigmoid-based probability calibration (e.g., Platt scaling). Such probability estimates, however, rely solely on global probability calibration and do not incorporate information about local label reliability, making them potentially sensitive to miscalibrated outputs.

Cost-sensitive SVM [4] is also introduced by Masnadi-Shirazi et al.. This line of work reformulates the SVM objective to incorporate class-dependent misclassification costs, enabling the classifier to adjust the decision boundary according to asymmetric error penalties. Such methods are particularly useful in imbalanced or risk-sensitive settings where one type of error is more costly than another. However, cost-sensitive SVMs operate at the class level and do not account for instance-wise reliability. As a result, they are unable to adapt to sample-specific noise or label uncertainty, limiting their effectiveness in scenarios where reliability varies within the same class.

For the KNN-based SVM, Zhang et al. proposed SVM-KNN [5], which integrates local neighborhood information into the SVM decision function. Their method first applies KNN to identify a sample’s local neighborhood and then uses this local structure to adjust the classification decision, effectively leveraging local class distributions to refine the SVM boundary. The core idea is to combine the global margin-maximizing property of SVM with locally adaptive decision rules derived from KNN. However, the method primarily focuses on modifying the decision rule rather than incorporating neighborhood reliability into the optimization process itself, and thus does not provide instance-specific weighting within the SVM loss formulation.

3 Method

Real-world datasets commonly suffer from two types of corruption: *feature outliers*, where samples lie far from the class distribution, and *label outliers*, where samples are assigned incorrect labels. Each type of noise affects the SVM optimization in different ways. To handle these outliers, we proposed three SVM models. The probability-weighted SVM (Prob-SVM) addresses feature outliers by introducing probabilistic term, p_i . However, Prob-SVM remains vulnerable to mislabeled samples because it does not consider local label consistency. Conversely, the KNN-based SVM (KNN-SVM) reduces the influence of label outliers by assigning knn-based term, n_i . but it does not account for feature-level deviations from the class distribution.

To jointly handle both types of noise, we introduce SKiP, which combines probabilistic reliability with KNN-based local consistency, leveraging the complementary strengths of both approaches.

3.1 Prob-SVM

The Naive-SVM minimizes Eq. (1), where all samples are penalized equally, making the model sensitive to outliers. To address this, we introduce a class-conditional probability weight $p_i = p(y_i)p(x_i | y_i)$, which scales each sample’s penalty by its posterior likelihood. The modified objective function is:

$$\min_{w,b} \frac{1}{2} \|w\|^2 + \sum_i C p_i \xi_i. \quad (2)$$

Here, inspired by LDA [6], the class-conditional likelihood $p(x_i | y_i)$ is estimated under a Gaussian assumption.

$$p(x_i|y_i) \sim \mathcal{N}(x_i | \mu_{y_i}, \Sigma_{y_i}).$$

However, for categorical features, outliers are unlikely to occur because their values are restricted to a fixed set of categories. Therefore, we set $p_{ij} = p(x_{ij}|y_i) = 1$ for categorical feature. This setting was applied to the Titanic dataset.

3.2 KNN-SVM

Although probability-weighted naive SVM improves robustness against feature outliers, it still relies solely on the reliability estimated from the probabilistic model. To additionally handle label outliers, we consider a simple KNN [7]-based variant, **KNN-SVM**, in which the instance-specific penalty is determined by the KNN consistency term n_i . The optimization problem becomes

$$\min_{w,b} \frac{1}{2} \|w\|^2 + \sum_i C n_i \xi_i, \quad (3)$$

subject to

$$y_i(w^\top x_i + b) \geq 1 - \xi_i, \quad \xi_i \geq 0.$$

here,

$$n_i = \frac{1}{K} \sum_{x_k \in \mathcal{N}_K(x_i)} \mathbb{I}(y_k = y_i),$$

where $\mathcal{N}_K(x_i)$ denotes the K nearest neighbors of x_i , and $\mathbb{I}(\cdot)$ is the indicator function. Samples surrounded by inconsistent labels receive lower weights, making the classifier less sensitive to local label outliers.

3.3 SKiP

To address both feature outliers and label outliers, we propose SKiP, a model that integrates a KNN-based local consistency term with a probability-based reliability term.

$$\min_{w,b} \frac{1}{2} \|w\|^2 + \sum_i C \left(\frac{p_i + n_i}{2} \right) \xi_i \quad (4)$$

subject to $y_i(w^\top x_i + b) \geq 1 - \xi_i, \quad \xi_i \geq 0,$

where p_i represents the class-conditional probability weight, and n_i is the KNN-based label consistency term.

The motivation of adopting an additive combination of p_i and rather than a multiplicative form is to enhance robustness against unreliable reliability estimates. Since p_i and n_i each capture different aspects of samples, an inaccurate assumption in either term can adversely affect the final weight. If the two were multiplied, such errors would be amplified and could lead to excessive down-weighting of samples. By using an additive formulation, the two measures can complement each other, preventing performance degradation caused by noise in only one of them and yielding a more stable and reliable weighting scheme.

To further support this design choice, we provide additional experiments in the Appendix C that compare alternative strategies for combining p_i and n_i . Specifically, we examine both additive and multiplicative formulations. Also, we examined rescaled p_i and n_i using min–max normalization to the range $[0, 1]$ before aggregation.

4 Experiments

4.1 Datasets

In this experiment, we use three base datasets: the Wine [8], Iris [6], and Titanic datasets [9]. The motivation for selecting these datasets is as follows: two of them (Wine, and Iris) exhibit moderately Gaussian-like feature distributions, whereas the Titanic dataset does not follow a Gaussian distribution and additionally contains categorical features.

In addition, computing the probabilistic term in our model requires estimating class means and variances for all features, which incurs a computational cost proportional to the number of features. Since the training complexity of a linear SVM scales as $O(nd)$, where n is the number of samples and d is the feature dimension, reducing the dimensionality is beneficial for both probability estimation and SVM optimization. Therefore, to obtain a consistent and efficient low-dimensional representation across datasets, we apply Principal Component Analysis (PCA) and retain components that explain 95% of the total variance. With these preprocessing steps and dataset configurations, we obtain a total of eight datasets used in our experiments.

4.2 Noise Injection

To systematically define noise within the data, we utilized the Mahalanobis distance relative to the normal distribution of each cluster. Specifically, we investigated the robustness of the SVM by introducing noise where $k\%$ of the original dataset is created to cross the decision boundary. We employed an arbitrary classifier, denoted as the `base_model`, to establish this decision boundary.

Consequently, we defined **Feature outliers** as data points that satisfy two simultaneous conditions:

1. The point’s Mahalanobis distance exceeds the 99th ($= \tau$) percentile of the cluster’s distribution.
2. The point crosses the decision boundary of the `base_model`.

This definition ensures that the injected noise represents statistically significant outliers that also disrupt the classification boundary.

Initially, we attempted to generate outliers using a naive rejection sampling strategy, where candidate points were iteratively generated and retained only if they exceeded the distance threshold. However, this approach proved computationally prohibitive due to the low acceptance probability of valid noise samples.

To mitigate this high computational cost, we introduced a **Cholesky-decomposed outlier injection** method. Unlike the iterative approach, this method directly constructs samples satisfying the distributional constraints, resulting in an approximate 100 times ($= \frac{1}{1-\tau}$) speedup. Detailed implementation and mathematical derivations are provided in Appendix A.

For **Label outliers**, we aimed to simulate label contamination within the dataset. To generate this noise, we randomly sampled $k\%$ subset of existing data points and flipped their class labels. Subsequently, we applied slight perturbations to these feature vectors to introduce marginal spatial deviations from the original instances.

4.3 Experiments

To evaluate the effectiveness of the proposed method, we conduct comparative experiments using four SVM variants: (1) the baseline naive SVM, (2) the probability-weighted SVM, (3) the KNN-weighted SVM, and (4) the proposed SKiP model, which incorporates both probabilistic and KNN-based weighting schemes.

We conducted experiments on three datasets (Iris, Wine, Titanic) with PCA, injecting noise levels ranging from 0% to 20% into both the labels and the feature space to simulate label corruption and feature outliers. Model performance was assessed by comparing the classification accuracy under these varying noise conditions. For all models, the regularization parameter C was selected from $\{0.1, 1, 10, 100, 1000, 10000\}$. For k -based methods such as KNN-SVM and SKiP-SVM, we

additionally tuned $k \in \{3, 5, 7, 10, 15\}$. Among all configurations, we report the performance achieved with the best-performing hyperparameter setting.

All experiments were conducted on a single server equipped with $2 \times$ AMD EPYC 9354 CPUs (32 cores / 64 threads each; 64 cores / 128 threads in total). With parallel computing enabled, the full experimental pipeline required approximately two hours to complete.

4.4 SVM Evaluation at Gaussian distribution (Iris, Wine Dataset)

Table 1: Classification accuracy under label and feature outliers on Iris and Wine datasets.

Dataset	Outlier (%)		Accuracy (%)				
	Label	Feature	Naive-SVM	Prob-SVM	KNN-SVM	SKiP	
Iris	0	0	86.7	86.7	90.0	93.3	
		10	87.9	75.8	81.8	84.8	
		20	80.6	86.1	91.7	88.9	
	10	0	80.0	80.0	83.3	83.3	
		10	78.8	69.7	81.8	87.9	
		20	75.0	66.7	81.8	83.3	
	20	0	63.3	70.0	70.0	70.0	
		10	69.7	66.7	72.7	75.0	
		20	63.9	66.7	72.7	75.0	
	Wine	0	0	100.0	100.0	100.0	100.0
			10	97.4	89.7	94.9	97.4
			20	93.0	88.4	90.7	93.0
10		0	83.3	83.3	86.1	83.3	
		10	92.3	84.6	86.0	94.9	
		20	93.0	86.0	89.7	93.0	
20		0	83.3	80.6	86.1	86.1	
		10	79.5	70.5	74.4	79.5	
		20	74.4	72.1	72.1	74.4	

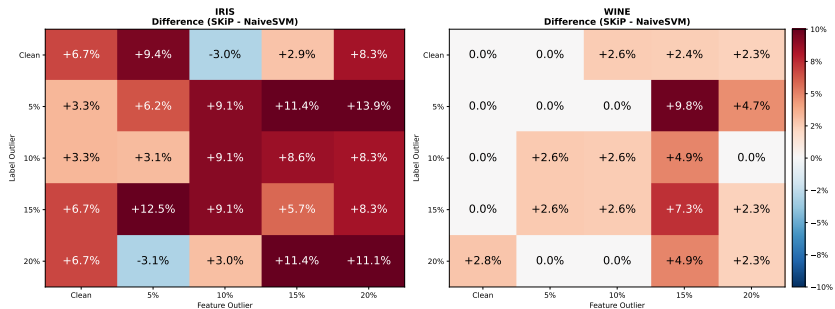


Figure 2: Accuracy difference (SKiP – Naive-SVM) under varying label and feature outlier levels on the *Iris* (left) and *Wine* (right) datasets.

As shown in Table 1, for both the Iris and Wine datasets, our SKiP model achieves the best performance across nearly all outlier configurations. Furthermore, as illustrated in Fig. 2, the SKiP model consistently outperforms the naive SVM across almost all batches.

In contrast to the naive SVM, both KNN-SVM and the SKiP variants exhibit a much smaller degradation in accuracy as noise levels increase. Although Prob-SVM often shows competitive performance, it suffers from sharp drops at certain noise combinations. This vulnerability, however, is largely dismissed in SKiP, since our formulation uses an additive weighting scheme rather than the multiplicative form used in Prob-SVM. As a result, SKiP is less sensitive to the cases where Prob-SVM experiences substantial performance loss.

Furthermore, in several regions—for example, the (10%, 10%) noise setting in the Iris dataset—both KNN-SVM and Prob-SVM show noticeable degradation, yet SKiP still achieves comparatively higher accuracy. This improvement arises from the fact that SKiP integrates the two complementary weights (local decision reliability and instance similarity) through addition, allowing it to retain robustness even when one of the individual components becomes unreliable. In such cases, the two weighting terms effectively compensate for each other, producing a synergistic effect that leads to more stable and resilient predictions under noise.

4.5 SVM Evaluation at Non-Gaussian distribution (Titanic Dataset)

Table 2: Classification accuracy under label and feature outliers on Titanic datasets.

Dataset	Outlier (%)		Accuracy (%)			
	Label	Feature	Naive-SVM	Prob-SVM	KNN-SVM	SKiP
Titanic	0	0	77.7	77.7	79.3	79.9
		10	74.0	73.5	74.5	74.5
		20	72.9	72.0	72.9	73.4
	10	0	72.1	72.1	72.6	73.2
		10	68.4	63.8	68.4	68.4
		20	59.8	57.5	67.8	67.8
	20	0	65.9	65.9	69.3	68.2
		10	63.8	60.7	65.8	64.8
		20	55.1	55.1	66.4	66.4

Interestingly, as shown in Table 2, despite the fact that the Titanic dataset deviates substantially from a Gaussian distribution, SKiP still exhibits stable and competitive performance. In contrast, Prob-SVM—whose probabilistic weighting scheme implicitly relies on Gaussian-like assumptions—shows notable degradation on this non-Gaussian dataset, particularly due to the presence of categorical features. One might therefore expect SKiP to inherit similar limitations, given that it incorporates the probabilistic reliability term from Prob-SVM. However, SKiP’s formulation is further reinforced by the KNN-based similarity component, which performs reliably on this dataset.

The robustness of SKiP becomes even more evident when examining the accuracy differences in Fig. 3. Across a wide range of label–feature noise combinations, SKiP consistently outperforms the naive SVM, often by a substantial margin—particularly in high-noise scenarios such as the (20%, 20%) setting. These improvements demonstrate that the two weighting mechanisms in SKiP operate in a complementary manner, enabling the model to maintain strong predictive accuracy despite significant distributional mismatch.

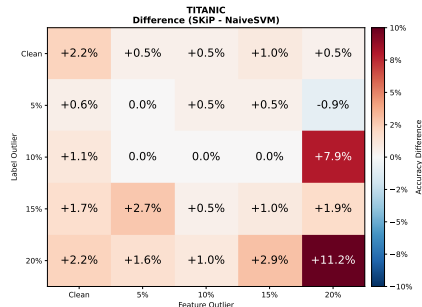


Figure 3: Accuracy difference (SKiP – Naive-SVM) under varying label and feature outlier levels on the *titanic*.

4.6 Stochastic Gradient Descent-based SKiP

Standard soft-margin SVMs inherently struggle with large-scale datasets due to their high computational complexity. To address this issue, Shalev-Shwartz et al. introduced a stochastic gradient-based (SGD) optimization algorithm for training SVMs called Pegasos [10].

Motivated by this, we conduct additional experiment to investigate whether the SKiP weighting mechanism can maintain its robustness and efficacy when integrated into this SGD framework for large-scale tasks.

Consistent with our previous experiments, we compared four SVM variants on the CIFAR-10 dataset [11]. In this experiment, due to the prohibitive computational cost of KNN on large-scale datasets, we adopted Approximate Nearest Neighbors (ANN). Consequently, the KNNSVM-SGD

model was replaced by the ANNSVM-SGD model. The detailed mathematical formulations and experimental configurations are provided in Appendix E.1.

Table 3: Classification accuracy under label and feature outliers on CIFAR-10 dataset.

Dataset	Outlier (%)		Accuracy (%)			
	Label	Feature	NaiveSVM-SGD	ProbSVM-SGD	ANNSVM-SGD	SKiP-SGD
CIFAR-10	0	0	36.7	36.7	33.9	37.6
		10	36.7	36.6	33.6	37.2
		20	36.0	36.0	33.4	37.1
	10	0	36.2	36.7	34.0	37.4
		10	36.8	37.1	34.6	37.6
		20	36.7	36.9	34.0	37.9
	20	0	36.9	37.1	34.2	37.2
		10	36.2	36.7	35.0	37.5
		20	36.5	36.8	34.8	37.7

As illustrated in Table 3, while the ANNSVM-SGD model suffers from significant performance degradation, the SKiP-SGD model demonstrates superior classification accuracy across all combinations of label and feature outliers on the CIFAR-10 dataset. A detailed analysis of why SKiP succeeds while ANNSVM-SGD fails on CIFAR-10 dataset is provided in Appendix E.2. Furthermore, SKiP maintains a clear and consistent performance advantage over the Naive SVM-SGD. In conclusion, this confirms that SKiP can be successfully scaled to large-scale datasets via the SGD approach without losing its inherent robustness against noise.

5 Conclusion

In this work, we introduced SKiP, a weighted SVM framework that integrates a probabilistic reliability term with a KNN-based local consistency measure to jointly address feature outliers and label corruption. Across Gaussian and non-Gaussian datasets, SKiP achieved consistently stable performance compared to Naive-SVM, Prob-SVM, and KNN-SVM, demonstrating the advantages of its additive weighting design. Also, further analysis of support vector structures detailed in Appendix D. showed that SKiP forms a balanced decision boundary without excessive sparsity or instability. Moreover, our experiments demonstrated that the SGD-based implementation of SKiP also yields meaningful performance improvements on large-scale datasets. Overall, SKiP provides a practical and robust extension of soft-margin SVM under diverse noise conditions.

Limitations Although SKiP demonstrates improved robustness across diverse noise conditions, several limitations remain.

First, the probabilistic component of SKiP is derived under a Gaussian assumption when estimating class-conditional likelihoods. Consequently, in datasets that deviate significantly from Gaussian behavior or contain substantial categorical structure, the reliability estimates may become less informative. While the additive integration with the KNN-based term alleviates this issue, SKiP still inherits a degree of sensitivity from its probabilistic foundation.

Second, the use of KNN-based (ANN-based) local similarity requires additional neighborhood computations during training. This process increases the overall computational burden compared to standard soft-margin SVM.

Nevertheless, despite these limitations, the design of SKiP allows it to retain strong robustness under label corruption and feature perturbations. This dual-weight structure enables SKiP to outperform conventional SVM variants in noisy or irregular settings, highlighting its effectiveness as a practical and resilient extension of soft-margin SVM.

References

- [1] M.A. Hearst, S.T. Dumais, E. Osuna, J. Platt, and B. Scholkopf. Support vector machines. *IEEE Intelligent Systems and their Applications*, 13(4):18–28, 1998.
- [2] Chun-Fu Lin and Sheng-De Wang. Fuzzy support vector machines. *IEEE Transactions on Neural Networks*, 13(2):464–471, 2002.
- [3] John Platt. Probabilistic outputs for support vector machines and comparisons to regularized likelihood methods. *Adv. Large Margin Classif.*, 10, 06 2000.
- [4] Hamed Masnadi-Shirazi, Nuno Vasconcelos, and Arya Iranmehr. Cost-sensitive support vector machines. *CoRR*, abs/1212.0975, 2012.
- [5] Hao Zhang, A.C. Berg, M. Maire, and J. Malik. SVM-KNN: Discriminative nearest neighbor classification for visual category recognition. In *2006 IEEE Computer Society Conference on Computer Vision and Pattern Recognition (CVPR'06)*, volume 2, pages 2126–2136, 2006.
- [6] R. A. Fisher. The use of multiple measurements in taxonomic problems. *Annals of Eugenics*, 7(2):179–188, 1936. doi: 10.1111/j.1469-1809.1936.tb02137.x.
- [7] Thomas Cover and Peter Hart. Nearest neighbor pattern classification. *IEEE transactions on information theory*, 13(1):21–27, 1967.
- [8] S. Aeberhard, D. Coomans, and O. de Vel. Comparative analysis of statistical pattern recognition methods in high dimensional settings. Technical Report Tech. Rep. no. 92-02, Department of Computer Science and Department of Mathematics and Statistics, James Cook University of North Queensland, 1994.
- [9] R. J. M. Dawson. The “unusual episode” data revisited. *Journal of Statistics Education*, 3(3): 1–14, 1995. Dataset: Titanic passenger survival data.
- [10] Shai Shalev-Shwartz, Yoram Singer, Nathan Srebro, and Andrew Cotter. Pegasos: Primal estimated sub-gradient solver for svm. In *Proceedings of the 24th International Conference on Machine Learning*, pages 807–814, 2007.
- [11] Alex Krizhevsky and Geoffrey Hinton. Learning multiple layers of features from tiny images. Technical Report 0, University of Toronto, Toronto, Ontario, 2009.
- [12] Yury A. Malkov and Dmitry A. Yashunin. Efficient and robust approximate nearest neighbor search using hierarchical navigable small world graphs. *CoRR*, abs/1603.09320, 2016.

Appendix

A Cholesky-decomposed outlier injection

Algorithm 1: Generation of Feature Outliers.

Input: Training data $(X_{\text{train}}, y_{\text{train}})$; feature-noise rate k

Output: Augmented dataset (\tilde{X}, \tilde{y})

Estimate, for each class c , the mean μ_c and covariance matrix Σ_c .

For each class c , compute a Cholesky factor $\Sigma_c = L_c L_c^\top$.

$N_{\text{noise}} \leftarrow k \cdot |X|$

for $i = 1$ **to** N_{noise} **do**

Select a class c uniformly at random.

Sample latent vector $z \sim \mathcal{N}(0, I_d)$.

Sample excess distance $E \sim \text{Exp}(2/\tau_c)$.

Compute target squared distance $\gamma^2 \leftarrow \tau_c + E$.

Calculate scaling factor $\alpha \leftarrow \sqrt{\frac{\gamma^2}{\|z\|_2^2}}$.

Construct outlying point $x_{\text{new}} \leftarrow \mu_c + L_c(\alpha \cdot z)$.

(if it crosses decision boundary) Append (x_{new}, c) to (\tilde{X}, \tilde{y}) .

return (\tilde{X}, \tilde{y})

Here, we use the decision boundary produced by the scikit-learn SVM implementation as our baseline.

The primary motivation for this transformation is to enable precise and efficient control over the outlier generation process. In the original feature space, directly modifying x to satisfy a specific Mahalanobis distance is non-trivial due to the covariance structure. However, the proposed transformation maps the complex Mahalanobis distance to the simple Euclidean norm in the latent space ($\|z\|_2^2$). This equivalence allows us to generate a random seed z , deterministically scale its magnitude to meet the outlier threshold, and transform it back to x , thereby guaranteeing the desired distance without iterative checking.

For the validity of the proposed noise injection algorithm, we must demonstrate that if a latent vector z is sampled from a standard normal distribution $\mathcal{N}(0, I)$, the transformation $x = \mu + Lz$ yields a random vector x that strictly follows the target distribution $\mathcal{N}(\mu, \Sigma)$.

Formally, we proved the following theorem:

Theorem 1. *Let $\Sigma \in \mathbb{R}^{d \times d}$ be a positive definite covariance matrix with Cholesky decomposition $\Sigma = LL^\top$, where $L \in \mathbb{R}^{d \times d}$ is a lower triangular matrix. If $z \in \mathbb{R}^d$ is a random vector following a standard normal distribution, $z \sim \mathcal{N}(0, I_d)$ where $I_d \in \mathbb{R}^{d \times d}$ is the identity matrix, and we define $x = \mu + Lz$ with $\mu \in \mathbb{R}^d$, then $x \in \mathbb{R}^d$ follows a multivariate normal distribution $\mathcal{N}(\mu, \Sigma)$.*

Proof. Let the probability density function (PDF) of the d -dimensional standard normal vector z be given by:

$$f_z(z) = \frac{1}{(2\pi)^{d/2}} \exp\left(-\frac{1}{2}z^\top z\right)$$

We define the affine transformation $x = \mu + Lz$. Since Σ is positive definite, L is invertible. Thus, we can express z as a function of x :

$$z = L^{-1}(x - \mu)$$

By the change of variables formula, the PDF of x , denoted as $f_x(x)$, is related to $f_z(z)$ by the Jacobian determinant of the inverse transformation:

$$f_x(x) = f_z(L^{-1}(x - \mu)) \left| \det\left(\frac{\partial z}{\partial x}\right) \right|$$

The Jacobian matrix of the transformation $z = L^{-1}(x - \mu)$ with respect to x is L^{-1} . Therefore, the Jacobian determinant term is:

$$\left| \det\left(\frac{\partial z}{\partial x}\right) \right| = |\det(L^{-1})| = \frac{1}{|\det(L)|}$$

From the property of determinants, $\det(\Sigma) = \det(LL^T) = \det(L) \det(L^T) = (\det(L))^2$. Consequently, $|\det(L)| = |\Sigma|^{1/2}$. Substituting this back into the equation:

$$\left| \det \left(\frac{\partial z}{\partial x} \right) \right| = \frac{1}{|\Sigma|^{1/2}}$$

Now, substituting $z = L^{-1}(x - \mu)$ into the exponential term of $f_z(z)$:

$$z^T z = (L^{-1}(x - \mu))^T (L^{-1}(x - \mu)) = (x - \mu)^T (L^{-1})^T L^{-1} (x - \mu)$$

Since $(L^{-1})^T L^{-1} = (L^T)^{-1} L^{-1} = (LL^T)^{-1} = \Sigma^{-1}$, the exponent simplifies to:

$$z^T z = (x - \mu)^T \Sigma^{-1} (x - \mu)$$

Finally, combining all terms, we obtain the PDF for x :

$$f_x(x) = \frac{1}{(2\pi)^{d/2} |\Sigma|^{1/2}} \exp \left(-\frac{1}{2} (x - \mu)^T \Sigma^{-1} (x - \mu) \right)$$

This is effectively the probability density function of the multivariate normal distribution $\mathcal{N}(\mu, \Sigma)$. \square

With Thm.(1), we can convert input data x into latent vector z , which follows normal distribution. Then, we can proceed to determine the scaling factor α required to project the latent vector z into the outlier region. By definition, a point is classified as Feature outliers if its squared Mahalanobis distance strictly exceeds the threshold τ (corresponding to the 99th percentile). For the transformed vector $z' = \alpha z$, this condition implies:

$$\|z'\|^2 = \|\alpha z\|^2 = \alpha^2 \|z\|^2 > \tau \implies \alpha > \sqrt{\frac{\tau}{\|z\|^2}}.$$

A naive approach to satisfy this inequality is to apply a minimal deterministic scaling, such as $\alpha = \sqrt{1.05\tau/\|z\|^2}$. However, this method forces the generated noise to concentrate excessively near boundary defined by the 99th percentile, failing to capture the diversity of outliers likely to be encountered in real-world scenarios.

To mitigate this issue and ensure a broader coverage of the feature space, we introduce a stochastic excess term E . We define the target squared distance γ^2 as the threshold τ augmented by E , where $E \sim \text{Exp}(\lambda)$. We calibrated the rate parameter λ of the exponential distribution so that the expected squared distance of the noise becomes $\frac{3}{2}\tau$. Deriving λ from this expectation constraint:

$$\mathbb{E}[\gamma^2] = \tau + \mathbb{E}[E] = \tau + \frac{1}{\lambda} = \frac{3}{2}\tau \implies \lambda = \frac{2}{\tau}.$$

Substituting this back, we obtain the final formulation for the robust scaling factor α :

$$\alpha = \sqrt{\frac{\tau + E}{\|z\|^2}}, \quad \text{where } E \sim \text{Exp}\left(\frac{2}{\tau}\right).$$

B Can feature outliers Improve SVM Performance?

Contrary to the common intuition that noise invariably degrades model performance, we empirically observed that injecting feature outliers occasionally resulted in higher classification accuracy compared to the baseline. We hypothesize that this improvement stems from a data-driven regularization effect, where the expanded variance of the training data leads to a more robust decision boundary. In this section, we provide a theoretical justification for this phenomenon.

B.1 Proof of Covariance Inflation via Noise Sampling

First, we demonstrate that the covariance of the injected feature outliers is strictly "larger" (in the positive definite sense) than the covariance of the original distribution.

Let the original data follow a distribution with mean μ and covariance Σ . The squared Mahalanobis distance is defined as $D^2 = (x - \mu)^T \Sigma^{-1} (x - \mu)$. The feature outliers are generated from the region where $D^2 > \tau$, with τ being a high threshold (e.g., the 99th percentile). To analyze the covariance structure, we apply a whitening transformation:

$$z = \Sigma^{-1/2}(x - \mu) \sim \mathcal{N}(0, I_d).$$

Under this transformation, the condition $D^2 > \tau$ is equivalent to $\|z\|^2 > \tau$.

Now, consider the covariance of the noise, denoted as $\text{Cov}(X \mid D^2 > \tau)$. Using the linearity of the covariance operator under affine transformations:

$$\text{Cov}(X \mid D^2 > \tau) = \Sigma^{1/2} \text{Cov}(z \mid \|z\|^2 > \tau) \Sigma^{1/2}.$$

Due to the spherical symmetry of the standard normal distribution, the off-diagonal elements of $\text{Cov}(z \mid \|z\|^2 > \tau)$ are zero. The diagonal elements are identical and can be derived from the expected squared norm. Since $\|z\|^2 = \sum_{i=1}^d z_i^2$, by symmetry:

$$\text{Var}(z_i \mid \|z\|^2 > \tau) = \mathbb{E}[z_i^2 \mid \|z\|^2 > \tau] = \frac{1}{d} \mathbb{E}[\|z\|^2 \mid \|z\|^2 > \tau].$$

For a standard normal distribution, the unconditional expectation is $\mathbb{E}[\|z\|^2] = d$. However, when conditioned on the tail region $\|z\|^2 > \tau$, the expected squared norm is strictly greater than the global mean:

$$\mathbb{E}[\|z\|^2 \mid \|z\|^2 > \tau] > \mathbb{E}[\|z\|^2] = d.$$

Consequently, the variance of the whitened noise components exceeds 1:

$$\text{Cov}(z \mid \|z\|^2 > \tau) = \beta I_d, \quad \text{where } \beta = \frac{1}{d} \mathbb{E}[\|z\|^2 \mid \|z\|^2 > \tau] > 1.$$

Mapping back to the original feature space, we obtain:

$$\text{Cov}(X \mid D^2 > \tau) = \beta \Sigma^{1/2} I_d \Sigma^{1/2} = \beta \Sigma \succ \Sigma.$$

This proves that the covariance of the injected noise is a scalar multiple of the original covariance, scaled by a factor $\beta > 1$, thereby strictly increasing the overall variance of the augmented dataset.

B.2 Connection to Margin and Generalization

The inflation of covariance directly impacts the Support Vector Machine (SVM) optimization. Consider the variance of the decision function projection for a weight vector w :

$$\text{Var}(w^T x) = w^T \Sigma w.$$

With the injection of Feature outliers, the effective covariance becomes $\tilde{\Sigma} \approx (1 - \rho)\Sigma + \rho(\beta\Sigma)$, which satisfies $\tilde{\Sigma} \succ \Sigma$, where ρ implies percentage of noise. This implies:

$$w^T \tilde{\Sigma} w > w^T \Sigma w.$$

Therefore, the causal chain of the performance improvement can be summarized as follows:

$$\Sigma \uparrow \longrightarrow \text{Var}(w^T x) \uparrow \longrightarrow \text{Margin} \uparrow \longrightarrow \text{Generalization} \uparrow.$$

In conclusion, the injection of Feature outliers acts as a robust mechanism for variance inflation, potentially preventing overfitting to the dense core of the distribution. However, it is crucial to note that this improvement is observed only in specific cases where the noise intensity is moderate.

The benefit of noise injection relies on a delicate balance. While moderate noise effectively expands the feature space and encourages a more generalized boundary, excessive noise can be detrimental. If the injected outliers are sufficiently aggressive to drastically alter the set of **Support Vectors (SVs)**, they may distort the optimal hyperplane rather than stabilizing it. Thus, feature outliers serves as a regularizer only when it inflates the data variance without fundamentally corrupting the structural integrity of the original support vectors.

C Ablation on SKiP Weight Aggregation Strategies

C.1 Experiments

For comparing SKiP model, we further implement four variants to examine different strategies for combining the probabilistic term p_i and the KNN-based term n_i . Specifically, we consider both multiplicative and arithmetic-mean formulations to investigate how the two weighting components interact. In addition, to ensure that the two terms have comparable influence, we also apply min–max normalization (scaling each term to the range $[0, 1]$), resulting in four SKiP variants.

C.2 Results

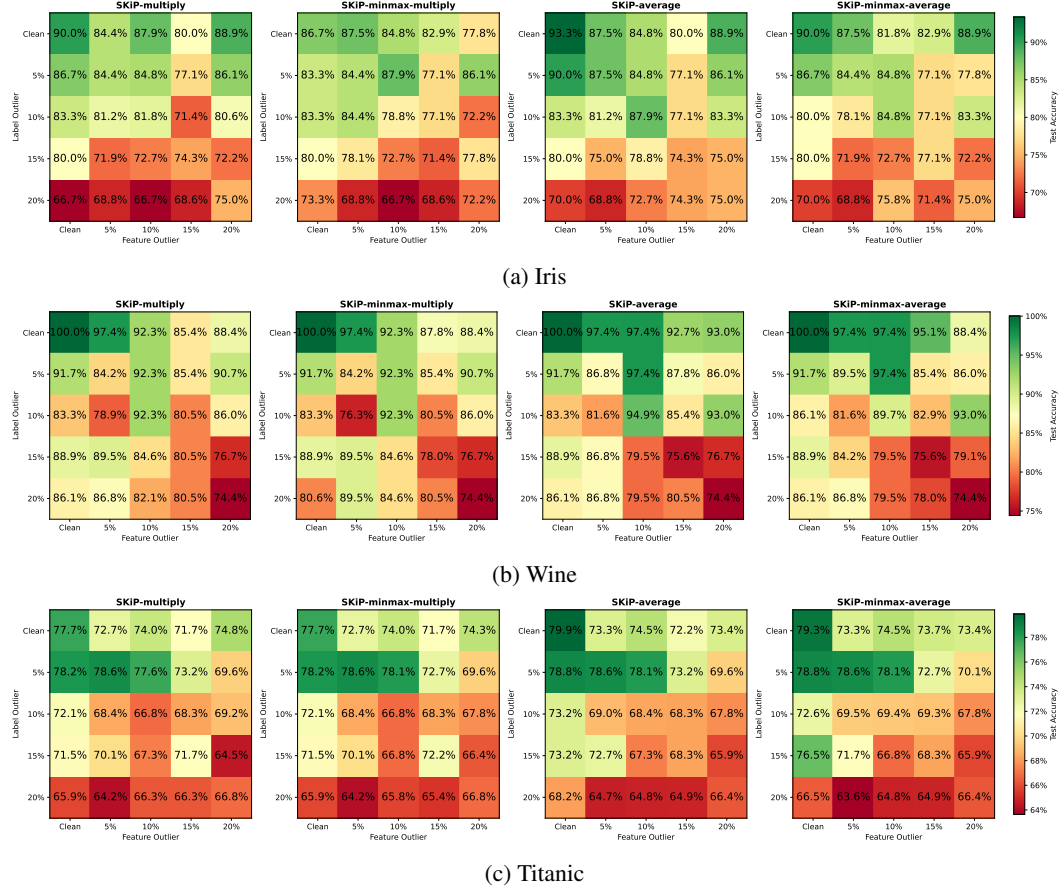


Figure 4: Evaluation of multiplicative, averaged, and min–max–normalized SKiP weighting schemes under label and feature perturbations across three datasets

- **SKiP–Multiply:** This variant directly uses the multiplicative form

$$C_i = C p_i n_i,$$

where the instance weight is defined as the product of the probability- and KNN-derived terms.

- **SKiP–MinMax–Multiply:** In this variant, both p_i and n_i are first scaled into the range $[0, 1]$ using min–max normalization, i.e., $\tilde{p}_i = \text{MinMax}(p_i)$ and $\tilde{n}_i = \text{MinMax}(n_i)$. The instance weight is then computed via

$$C_i = C \tilde{p}_i \tilde{n}_i.$$

- **SKiP–Average(baseline):** This variant employs the arithmetic mean of the two terms:

$$C_i = C \frac{p_i + n_i}{2}.$$

- **SKiP–MinMax–Average:** Here, the min–max normalized terms \tilde{p}_i and \tilde{n}_i , each rescaled to the interval $[0, 1]$, are averaged to obtain

$$C_i = C \frac{\tilde{p}_i + \tilde{n}_i}{2}.$$

In Figure 4, we can observe that the multiply formulation tends to be unstable: because the final weight is defined as the product of the probabilistic reliability and the KNN-based similarity, poor performance in either component substantially degrades the combined weight. As a result, when the probabilistic term becomes unreliable—for example, in non-Gaussian datasets such as Titanic—the multiply scheme fails to leverage the stronger KNN term, leading to inconsistent performance across noise levels.

In contrast, the average formulation shows noticeably more robust and stable performance across all datasets. Since the two components contribute additively, this scheme avoids the “weakest link” issue inherent in the multiplicative design and allows one component to compensate when the other becomes unreliable.

The min–max variants exhibit only marginal differences from their unnormalized counterparts. While min–max normalization adjusts the scale of each weighting component, it does not meaningfully alter relative sample ordering, which explains the minimal performance change. Nevertheless, the use of min–max normalization introduces a potential concern, and its practical implications should be interpreted with caution.

C.3 Potential Issues with Min–Max Scaling

In SKiP, the weight p_i is defined as a Gaussian-based probability assigned to each data point. Since it is a probability induced by the normal model, it necessarily satisfies

$$0 < p_i < 1.$$

Our concern is not the boundedness of p_i itself, but what happens when min–max scaling is applied to these values. Min–max normalization uses the empirical extrema of the dataset,

$$\tilde{p}_i = \frac{p_i - p_{\min}}{p_{\max} - p_{\min}}, \quad p_{\min} = \min_j p_j, \quad p_{\max} = \max_j p_j,$$

and forces the smallest observed Gaussian probability to become exactly zero:

$$p_i = p_{\min} \Rightarrow \tilde{p}_i = 0.$$

This implies that if a new point x_j is drawn such that it lies farther from the class mean than the most extreme sample in the training set, then its Gaussian-based probability can become smaller than the empirical minimum. Consequently,

$$p_j < p_{\min} \Rightarrow \tilde{p}_j < 0 \Rightarrow \tilde{p}_j = 0 = \tilde{p}_i,$$

So, as a result, using min–max scaling can disrupt the assumption that p_i is drawn from a Gaussian-based probability distribution. Even when we adopt a practical safeguard by imposing a numerical floor,

$$p_i < 10^{-6} \Rightarrow p_i = 10^{-6},$$

this does not fully resolve the issue. Such clipping merely prevents extremely small probabilities from becoming numerically indistinguishable from zero, but it cannot restore the original Gaussian-derived semantics once the min–max transformation anchors the empirical minimum at $\tilde{p} = 0$ and makes the scale dataset-dependent. Therefore, the resulting weights should still be interpreted as relative scores rather than model-consistent probabilities.

D Support Vector Analysis

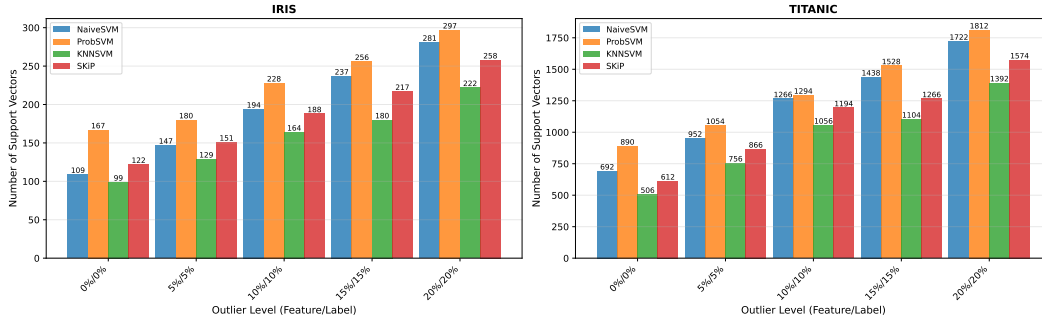


Figure 5: Comparison of the number of Support Vectors (SVs) across varying noise levels on Iris and Titanic datasets.

To further understand the structural differences among the weighting schemes, we analyze the number of support vectors (SVs) produced by each method. In the dual formulation of soft-margin SVMs, each sample satisfies the box constraint

$$0 \leq \alpha_i \leq C_i, \quad (5)$$

and becomes a support vector whenever $\alpha_i > 0$. Points with $0 < \alpha_i < C_i$ lie on the margin, whereas $\alpha_i = C_i$ indicates a point inside the margin or a misclassified sample. Thus, the per-sample upper bound C_i has a direct structural influence on SV formation: reducing C_i restricts the feasible range of α_i , and if the unconstrained optimum would exceed the reduced bound, the constraint becomes active and the sample becomes an SV. Furthermore, due to the dual feasibility condition

$$\sum_i \alpha_i y_i = 0, \quad (6)$$

adjusting C_i for one sample reshapes the optimal distribution of α_j across other samples, so the number of SVs does not change monotonically with C_i and may increase or decrease depending on the data geometry.

From this viewpoint, the observed differences among methods can be interpreted through their weighting structures. The KNN-based weighting n_i exhibits a *discrete-like* behavior: samples whose local neighborhoods disagree with their labels often yield n_i values that are very close to zero. Since each method enforces the constraint $\alpha_i \leq C n_i$, the probability that $C_i = C n_i$ becomes extremely small is relatively high. Consequently, many ambiguous or noisy points are effectively suppressed, contributing little to the decision boundary and resulting in the smallest number of SVs among the compared methods.

In contrast, the probabilistic weighting p_i is derived from Gaussian class-conditional likelihoods. Because Gaussian densities are continuous and rarely collapse to exactly zero—even in high-dimensional settings—the resulting weights satisfy $p_i > 0$ almost surely after normalization. Thus, the effective bounds $C_i = C p_i$ seldom become extremely small. Combined with the dual coupling constraints, this continuous structure often leads to a larger number of active constraints and therefore to a larger number of SVs, sometimes even exceeding the Naive-SVM despite the fact that $C_i \leq C$ for all samples.

The SKiP method occupies an intermediate position. When using the averaging rule

$$C_i^{\text{SKiP}} = C \cdot \frac{p_i + n_i}{2}, \quad (7)$$

samples strongly suppressed by KNN-SVM (i.e., $n_i \approx 0$) receive partially restored weights through the influence of the continuous probabilistic term p_i , while highly representative samples with both large p_i and n_i retain large effective bounds. This mixture prevents the extreme sparsification characteristic of KNN-SVM, yet avoids the broad activation pattern of Prob-SVM. As a result, the number of SVs produced by SKiP consistently lies between those of the KNN-based and probabilistic models.

Overall, the SV statistics reflect fundamental differences in how each weighting scheme manages noisy or ambiguous samples and constructs the resulting decision boundary. These patterns highlight that SV analysis provides a meaningful lens through which to interpret the behavior of weighted SVM formulations.

E Stochastic Gradient Descent-based SKiP

E.1 Method and Experimental Settings

Shalev-Shwartz et al. introduced a stochastic gradient-based optimization algorithm for training SVMs called **Pegasos** [10]. At each iteration t , Pegasos selects a training sample (x_t, y_t) and performs a stochastic subgradient update with learning rate $\eta_t = 1/(\lambda t)$:

$$w_{t+1} = \begin{cases} (1 - \eta_t \lambda) w_t + \eta_t y_t x_t, & \text{if } y_t(w_t^\top x_t) < 1, \\ (1 - \eta_t \lambda) w_t, & \text{otherwise.} \end{cases}$$

As a practical extension for large-scale applications, we integrated our SKiP weighting mechanism into the Pegasos framework. Let p_t denote the probabilistic reliability weight (as in Prob-SVM) and n_t denote the KNN-based similarity weight. SKiP combines these two components additively, so we define coefficient α_t :

$$\alpha_t = \frac{p_t + n_t}{2}.$$

By incorporating α_t into the update, the Pegasos step becomes

$$w_{t+1} = \begin{cases} (1 - \eta_t \lambda) w_t + \eta_t \alpha_t y_t x_t, & \text{if } y_t(w_t^\top x_t) < 1, \\ (1 - \eta_t \lambda) w_t, & \text{otherwise.} \end{cases}$$

Datasets For this experiment, we utilized the CIFAR-10 dataset, a 10-class image classification benchmark consisting of 50,000 training and 10,000 test samples. Given its high dimensionality as an image dataset ($32 \times 32 \times 3$), we applied Principal Component Analysis (PCA) and retained 256 components, following the same preprocessing approach as in our previous experiments. Furthermore, the noise injection for the CIFAR-10 dataset was conducted using Algorithm 1 in Appendix A. It should be noted, however, that due to the lower baseline accuracy of CIFAR-10 compared to previous datasets, using the base model for noise generation became unreliable. Therefore, we omitted base model’s boundary-crossing requirement (Condition 2) in generation of feature outliers for CIFAR-10 dataset. Consequently, feature outliers for CIFAR-10 were generated based solely on the Mahalanobis distance criterion.

Experiment Settings To prevent multivariate Gaussian probabilities from vanishing in high dimensions, the weight p_t was computed using only the top p principal components from PCA. In this experiment, we set $p = 32$. Also, regarding the KNN-based similarity weight n_t , computing exact k-nearest neighbors becomes computationally prohibitive for the CIFAR-10 dataset due to its large scale of 50,000 training samples. To mitigate this excessive computational overhead, we employed an **Approximate Nearest Neighbor (ANN)** technique for calculating n_t , enabling efficient and scalable neighborhood search without severely compromising accuracy. For this experiment, we used **HNSW** [12] algorithm.

To evaluate the effectiveness of the proposed method, we conduct comparative experiments using four SGD-based SVM variants: (1) the baseline naive SVM (NaiveSVM-SGD), (2) the probability-weighted SVM (ProbSVM-SGD), (3) the ANN-weighted SVM (ANNSVM-SGD), and (4) the proposed SKiP model (SKiP-SGD), which incorporates both probabilistic and KNN-based weighting schemes.

Due to computational constraints, a random subsample of 10,000 training samples was drawn for each experiment. Noise was injected at levels ranging from 0% to 20% across both Feature outlier and Label outlier noise, with fractions drawn from {0%, 10%, 20%}, yielding a 3×3 grid of 9 noise conditions. Model performance was assessed by comparing test classification accuracy under these varying noise conditions.

All models were trained using mini-batch stochastic gradient descent with a linear kernel, regularization parameter $C = 1.0$ ($\lambda = 1/C = 1.0$), learning rate $\eta_t = 1/\lambda t$, 50 training epochs, and a mini-batch size of 256. For ANN-based methods (ANNSVM-SGD and SKiP-SGD), approximate nearest neighbor search was performed using a HNSW index with $k = 10$.

E.2 Why Does ANNSVM-SGD Underperform on the CIFAR-10 Dataset?

As shown in Table 3 of Section 4.6, ANNSVM-SGD underperforms compared to other models. In this section, we further investigate this issue.

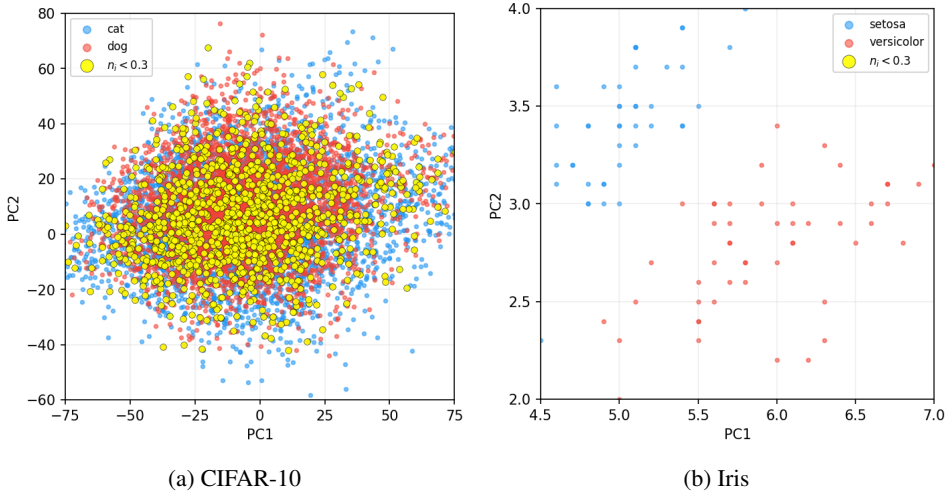


Figure 6: Data representation in the top-2 principal components (PCA) space of CIFAR-10, Iris dataset. Yellow points represent data with ANN-based weights lower than 0.3. ($n_i < 0.3$)

To investigate this issue from the perspective of dataset characteristics, we projected the data onto a PCA space and evaluated the ANN-based weights (n_i). Figure 6 shows that the cause of the ANNSVM-SGD model’s underperformance on CIFAR-10 lies in the severe class overlap within the feature space, which prevents the data from being linearly separated.

Table 4: Comparison of constraint weight between the Iris and CIFAR-10 datasets.

Class	N	n_i		p_i		$(n_i + p_i)/2$	
		≤ 0.01	Mean	≤ 0.01	Mean	≤ 0.01	Mean
Iris Dataset							
setosa	50	0.0%	1.000	0.0%	0.999	0.0%	0.999
versicolor	50	0.0%	0.918	0.0%	0.998	0.0%	0.958
virginica	50	0.0%	0.915	0.0%	0.997	0.0%	0.956
ALL (Iris)	150	0.0%	0.944	0.0%	0.998	0.0%	0.971
CIFAR-10 Dataset (PCA-256)							
airplane	5,000	11.3%	0.406	0.0%	0.994	0.0%	0.700
automobile	5,000	40.0%	0.174	0.0%	0.996	0.0%	0.585
bird	5,000	8.4%	0.321	0.0%	0.994	0.0%	0.657
cat	5,000	25.3%	0.173	0.0%	0.996	0.0%	0.584
deer	5,000	7.6%	0.400	0.0%	0.995	0.0%	0.698
dog	5,000	27.5%	0.201	0.0%	0.995	0.0%	0.598
frog	5,000	10.9%	0.321	0.0%	0.995	0.0%	0.658
horse	5,000	30.8%	0.221	0.0%	0.995	0.0%	0.608
ship	5,000	7.0%	0.544	0.0%	0.995	0.0%	0.769
truck	5,000	39.7%	0.160	0.0%	0.996	0.0%	0.578
ALL (CIFAR-10)	50,000	20.9%	0.292	0.0%	0.995	0.0%	0.644

Unlike the Iris dataset, this complex and non-linear distribution in CIFAR-10 leads to a drastic degradation in n_i . The yellow points in the left panel of Figure 6 clearly show a massive concentration of original data with low weights ($n_i < 0.3$). Furthermore, Table 4 demonstrates that the overall mean of n_i for the CIFAR-10 dataset is extremely low at 0.292, with 20.9% of the CIFAR-10 instances receiving near-zero weights ($n_i \leq 0.01$). In the standard ANNSVM-SGD model, these near-zero values practically vanish and fail to act as meaningful constraints during the SVM margin optimization. Consequently, the model lacks the necessary constraint information to construct an accurate decision boundary, leading to significant performance degradation.

In contrast, our proposed SKiP method successfully mitigates this vulnerability by utilizing an additive operation, $(n_i + p_i)/2$, to formulate the final constraint weights. As shown in Table 4, while the n_i values collapse, the SKiP method restores the overall mean weight to 0.644. This enables the model to retain challenging samples that would be discarded due to near-zero n_i values in the ANNSVM-SGD model, allowing n_i to act as a valid contribution to the final constraint weight.

Therefore, proposed SKiP formulation prevents unintended sample exclusion and enables robust classification even in highly non-linear domains.

F Other Model Comparison

In this section, we compare SKiP with several classical classifiers, including KNN, decision trees, and logistic regression, using an RBF-kernel SVM setup. As shown in Table 5, adopting the RBF kernel enables the SVM-based models to operate with expressive capacity comparable to nonlinear baselines such as KNN and decision trees, providing a fair evaluation across heterogeneous model classes. This setting further verifies that the SKiP framework is naturally compatible with kernelized SVMs and consistently retains its performance advantages beyond the linear case.

Table 5: Performance comparison of baseline models and SVM variants under noise perturbations.

Dataset	Outlier (%)		Accuracy (%)			
	Label	Feature	KNN	Decision Tree	Logistic Regression	SKiP
Iris	0	0	96.7	86.7	93.3	93.3
		10	84.8	81.8	81.8	84.8
		20	83.3	88.9	88.9	86.1
	10	0	83.3	86.7	86.7	86.7
		10	81.8	84.8	81.8	84.8
		20	80.6	83.3	83.3	80.6
	20	0	66.7	70.0	66.7	70.0
		10	66.7	75.8	66.7	66.7
		20	69.4	72.2	75.0	69.4
Wine	0	0	97.2	94.4	100.0	100.0
		10	97.4	79.5	97.4	100.0
		20	93.0	83.7	95.3	93.0
	10	0	80.6	80.6	83.3	83.3
		10	89.7	79.5	92.3	94.9
		20	86.0	74.4	90.7	90.7
	20	0	80.6	80.6	83.3	83.3
		10	74.4	74.4	79.5	84.6
		20	72.1	65.1	69.8	76.7
Titanic	0	0	83.8	81.0	81.6	82.7
		10	81.1	80.1	74.5	82.7
		20	79.9	76.6	68.2	81.8
	10	0	76.0	76.0	72.1	73.2
		10	74.5	73.5	65.8	74.5
		20	72.9	74.3	62.6	72.0
	20	0	64.8	65.4	67.0	69.3
		10	67.3	67.3	66.3	71.4
		20	71.5	69.6	56.1	71.0